Application of Ant Colony Algorithm to the Analysis of High Frequency Equivalent Circuit of DC Motor

JINFENG LIU, XUDONG WANG
School of Electrical & Electronic Engineering, Harbin University of Science & Technology
52 Xuefu Road, Nangang District, Haerbin City, CHINA, ljf78118@163.com
NAN JIANG
Department of Electrical and Computer Engineering, Stevens Institute of Technology
Castle Point on Hudson, Hoboken NJ 07030-5991, UNITED STATES, njiang@stevens.edu

Abstract: - The Electromagnetic Compatibility (EMC) of direct current (DC) motor windings is a system model which is able to reflect the functional characters of the system in the whole EMC specified frequency(150KHz~30MHz). For most motor designing process, it always evaluated the inductance of windings in lower or working frequency; however, when analyzing the conducted interference, it is necessary to take some parameters in high frequency into account in building up the EMC model, such as the noticeable distributed capacitance among the windings or between windings and shells. Past research neglected the common-mode current generated by the high frequency interference through motor bearings coupled with shells, since the parasitic capacitance of rotor core comes from armature windings supplied sufficient paths. In EMC modelling for DC motor problem, first test the impedance of windings by experiments, then generate the equivalent circuit with total parameters. At present, it is a difficulty that how to choose the parameters. Most researchers preferred to adopt analytical calculation, however, it could not reflect the essence of the model since it requires many simplification. As a result, this paper adopted ant colony algorithm (ACA) with positive feedback to intelligent search and global optimize parameters of equivalent circuit. Simulation result showed that impedance of equivalent circuit calculated by this algorithm was the same as experimental result in the whole EMC frequency. In order to further confirm the validity of ACA, PSPICE circuit simulation was adopted to simulate the spectrum of common mode Electromagnetic Interference (EMI) of equivalent circuit. The simulation result accorded well with the experiment result received by EMI receiver. So it sufficiently demonstrated correctness of ACA in the analysis of high frequency equivalent circuit.

Key-Words: - Ant colony algorithm, Motor windings, EMC, Conducted interference, Common mode EMI, PSPICE simulation, EMI receiver

1 Introduction

As the development of communication technology, computer science, automatic control, vehicles, household appliance, electric power industry and military, the requirement of DC motors increased significantly. Since it is the key component in the domains mentioned above, the types and quantity of DC motors improved rapidly. At the same time, the structure and control of DC motors has changed significantly. However, as the key component of many systems (such as electrical vehicles and forklift), the DC motors have become the serious inner interference source of these systems, since when it operates, during the steering process and the unstable touch between brush and commutator there will generate transient voltage on the wires. These transient voltages will invade into other component as conducted interference through conductor [1-2]. As a result, it is essential to build up the correct high frequency model of DC motors for the improvement of electromagnetic compatibility of the system.

2 The generation of electromagnetic interference in separated exciting DC motor

The electromagnetic interference of separated exciting DC motor mainly comes from mutational electromagnetic in its windings and the electric arc between commutator and brush. In the steering process of motors with brushes, since when the brush moves from one commutator to another there would be contact resistance which change rapidly, the current would mutate into electric arc. Therefore, there will be impulsion field wave and these pulse interferences will become high frequency transient voltage on the wires than it will be conducted into other electrical systems and disturb the operation of their sensitive elements. Especially when the frequency of conducted interference is high enough, it will generate radiation through the antenna and aggravate the

electromagnetic environment of the whole system. These interferences are between the frequencies of 10 Hz to 1000 MHz, a quite wide frequency bandwidth [3].

When cutting off the current of motor windings, the electromagnetic field in the coils would disappear suddenly and a transient voltage with hundreds of, even thousands of voltage would be generated in the coils. This high voltage is quite similar to the exponential decay curve of first order circuit. Accordingly, this impulsion voltage would cause serious energy leakage and plunge into the control circuit then turn into huge electrical punch. When the motor operates in rated load, if the power supply to windings would be cut suddenly, the armature would continue working. Under the electromagnetic function of stator, windings of rotor will generate induction electromotive force combined with the original ones, then turned into over-voltage and its instantaneous peak could be 6-8 times than rated voltage. Finally, this over-voltage could decrease exponentially until armature stop rotating.

The peak of motor interference is related the typical structure of motor, normal workload, insulating aging of windings and the gap between commutator and brushes. In order to build up the simulate model of conducted electromagnetic interference of motor, it is necessary to analyze the generation of that interference and then build up the high frequency model of motor windings. Figure 1 shows the voltage wave of XQ-7A2 separately excited DC motor working in low rotational speed extracted by oscilloscope. From this figure, we could find that the voltage does not only oscillate periodically, but also has peak impulsion.

Many scholars have proved that the steering process of DC motor with brush is the essential source of electromagnetic interference and built up the simulation model of conducted interference by the analysis of steering process; however, this model is only accurate in low frequency, not suitable for high frequency of 150 KHz ~ 30 MHz which is regulated by standard CISPR14-1 : 2003. Consequently, it is necessary to build up an equivalent circuit to describe the common-mode characters in high frequency of DC motors. On one hand, it allows us to analyze the common-mode characters of DC motors without the specific experiment; on the other hand, it could be used to predict the conducted common-mode EMI of concrete driving system when system couldn't be measured by Line Impedance Stabilizing Network(LISN).

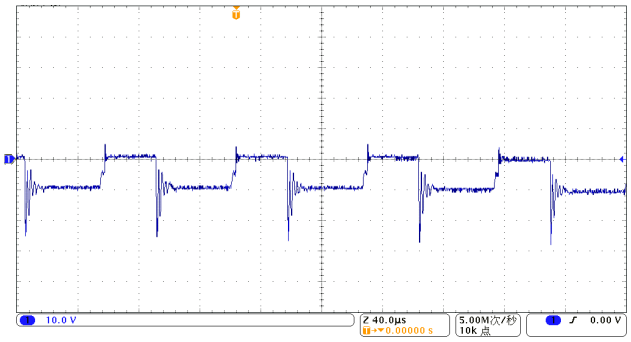

Fig.1 Terminal voltage waveform of DC motor

This paper takes the separately excited DC motor produced by Liaoning motor maker as example to build up the EMC model. In this process, besides building up the physical model according to motor characters, we need to set up the parameters of each element in it. This paper adopted Ant Colony Algorithm to determine the parameters in model. This Algorithm is a new distributing evolution algorithm. It has strong ability in solution searching, adaptability and robustness; it could also optimize the parameter collection process and make the impedance of equivalent circuit in model equal to measured value.

3 EMC model of separately excited DC motor windings

The common-mode equivalent circuits mentioned in [4] and [5] are applied to analyze and predict the over voltage on motor, shaft voltage/ current and other negative effect generated by common-mode voltage. Even use it to analyze the common-mode circuit for leakage current, it is only effective in frequency lower than 1MHz, hard to face the requirement of EMI of whole conducted interference frequency (150K~30MHz). The main difference between the high frequency common-mode equivalent circuit of separately excited DC motors and that of former ones is this model could be used to analyze and predict the emission intensity of common-mode EMI and motor side common-mode EMI current in the whole conducted interference frequency.

3.1 The common mode current coupled path of separately excited DC motor

The excitation and armature windings in the slots of stator and rotor inside separately excited DC motor are symmetrically distributed around the circle, while there are electromagnetic and electrical field inside the motor. That makes the DC motor has plenty of electromagnetic coupling inside and

applied sufficient path for high frequency EMI noise. Though there are many parasitic parameters in motors, considered the separated power supplement for excitation and windings and the speed control of motor is achieved by PWM controller on windings, the armature windings is the main component of the system to generate high frequency common mode EMI. Accordingly, the parasitic capacity is mainly achieved by analyzing the armature windings. There are mainly 3 types of parasitic capacity, the capacity from armature windings to rotor core (C_{sa}), the capacity from armature windings to stator core (C_{sf}), and the capacity from excitation windings to stator core (C_{sg}). According to the distribution of parasitic parameters of separately excited DC motor, the common mode current coupling path is showed in figure 2.

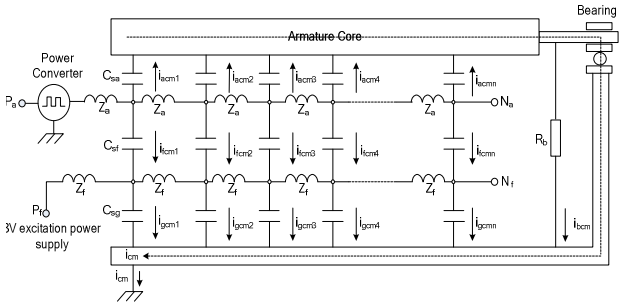

Fig.2 Common mode current coupled path inside separately excited DC motor

In figure 2, Z_a and Z_f represents the resistance of unit length of armature and excitation windings, respectively. R_b is the resistance of bearing, P_a and N_a, P_f and N_f is the positive and negative node of power supplement to armature and excitation windings, respectively, while the supplement to armature windings is achieved through the power converter. i_{cm} is large input common mode current, i_{acmk}, i_{fcmk}, i_{gcmk} (while k=1,2,…,n) is the common mode current of related parasitic capacity flows each length unit. By the analysis of the distribution of parasitic capacity inside the motor showed in figure 2 and motor structure, armature winding is affected most serious by high frequency interference, while excitation windings are affected less when working under high quality power supplement. Therefore, we can neglect the effect of excitation windings to common mode current and only take parasitic capacity into account when analyze common mode current path.

3.2 EMC model foundation of separately excited DC motor

The most effective method in researching high frequency characters of motor windings is multi-conductor and multi-element conducting model. For specified DC motor, armature core is homogeneous media in all directions, each rotor slot shares the same structure, winding turns and wire diameter are specified, as a result, motor windings could be considered as a uniform conductor. In analyzing and predicting the high frequency common-mode motor side current of DC motors, we could adopt lumped parameter model since it is simplified. [6] and [7] adopted this method and got acceptable result. This paper built up the EMC model of DC motor windings based on the analysis of separately excited DC motor accorded to former work, which is showed in figure 3.

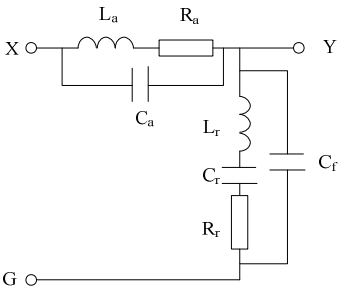

Fig.3 High frequency common mode equivalent circuit of separately excited DC motor

In figure 3 L_a is the common-mode inductance and C_a is parasitic capacity of armature windings; R_a is the sum of eddy current effect of core and resistance of armature windings; L_r is impedance of armature core; C_r is the sum of parasitic capacity between armature windings and rotor slot and parasitic capacity among armature core laminations; R_r is the sum of resistance of armature laminations and resistance of motor bearing; C_f is the parasitic capacity of armature windings coupled to excitation windings core. After had this equivalent circuit, we move on to calculate each parameter above according to given characters of motor. Here we use Ant Colony Algorithm.

For the equivalent circuit showed in figure 4, accorded to circuit theory, it is easy to get the expression of resistance of windings Z_{XY} and the common-mode resistance to earth Z_{XG} as following:

$$Z_{XY}(s) = \frac{R_a + sL_a}{1 + R_a C_a s + L_a C_a s^2} \quad (1)$$

$$Z_{XG}(s)=\frac{R_a+sL_a}{1+R_aC_as+L_aC_as^2}+\frac{1+R_rC_rs+L_rC_rs^2}{(C_r+L_r)s+R_rC_rC_fs^2+L_rC_rC_fs^3} \quad (2)$$

4 Ant colony algorithm

Ant Colony Algorithm, ACA, is a new evolution simulated algorithm applied in 90s of 20th century. Similar to genetic algorithm, simulated annealing algorithm and other simulated evolution, it searches the optimized solution through the evolution process of the group combined by candidate solution. This algorithm adopts positive feedback mechanism in order to implement intelligent searching and global optimization; meanwhile, it has strong robustness [8].

Although the parameters of high frequency interference model of DC motor could be received by mathematical computation, these parameters are not accurate because of predigestion and estimation of existence. We could consider that parameters are optimized base on solution space received by mathematical analysis, and ACA is well suited to this optimization process. The construction process of ACA solution is a course finished step by step. This algorithm may turn the prior knowledge based solution space to full account and deal with constrained conditions conveniently in this course. Ants could modulate dynamically next junction that can be referred in construction process, so it will guarantee accuracy and feasibility of solution. This algorithm has the ability of distributed parallel computation and avoids local optima like other algorithm. ACA is not fastest algorithm but it's relative more accurate algorithm [9].

4.1 Principle of ACA

Suppose there are m parameters to optimize, denoted as p1, p2, …, pm, for any one among them pi ($1 \leqslant i \leqslant m$), set it as N possible non-zero value, combined set Qp_i. Then, all the ants leave the formicary for food, and each ant starts from set Qp_i, based on the pheromone $\tau_j(Qp_i)$ of each element in set and state transition probability $P(\tau_j^k(Q_{P_i}))$, randomly choose one and only one element in set Qp_i independently. State transition probability and pheromone are calculated by (3) and (4), respectively.

$$P(\tau_j^k(Q_{P_i}))=\frac{\tau_j(Q_{P_i})}{\sum_{g=1}^{N}\tau_g(Q_{P_i})} \quad (3)$$

$$\tau_j(Q_{P_i})(t+n)=\rho\tau_j(Q_{P_i})(t)+\Delta\tau_j(Q_{P_i}) \quad (4)$$

Where ρ is the duration indice of residue information and 1-ρ is the volatility. $\Delta\tau_j(Q_{P_i})$ is the increased pheromone on jth element caused by all the ants in this loop. This increase is determined by the difference of analytical and concrete output, the smaller the difference is, the more the pheromone increases[10].

After all ants finished choosing elements in the set, they get the food source. Then adjust the pheromone of each element. This process will be repeated until the optimized solution be found or reach the iteration times [11].

4.2 Parameter selection based on ACA

The mechanism of ACA path searching shows that there is essential effect from parameter selection to the performance of ACA. However, there is no theoretical basis for parameter setting and to get the optimized solution by experience through repeated matching and adjust. The scale of solution space N and number of ants K are close related to the efficient of optimized solution searching, accuracy and global superiority of solution, and other optimization function. If the optimized solution is dense in parts, it is better to choose large N. The selection of K is related to N, the larger N is, the lager K is required, meanwhile, it should take the time complexity of the algorithm into account in the selection of K[12]. Normally, the duration indices of residue information are $0.5 \leqslant \rho \leqslant 1$ and 0.7 is optimized; total pheromone value Q is $1 \leqslant Q \leqslant 10000$ and has little effect to algorithm. Since the selection range of Q is much larger than that of ρ, in practical, we set ρ randomly first, than calculate the value of Q; after get a value of Q, readjust ρ in order to get a more optimized solution. Repeat this process by times, the optimized parameter group would be finally reached [13].

4.3 Implementation of ACA in EMC modeling of DC motor

Figure 4 shows the flowchart of setting the parameter in equivalent circuit using ACA.

The common-mode current equivalent circuit of separately excited DC motor shows that there are 7 parameters need to set by ACA. According to the characters of motor, set up the candidate solution group (7×30), that is the set Qp_i required by ACA, where m=7, N=30.

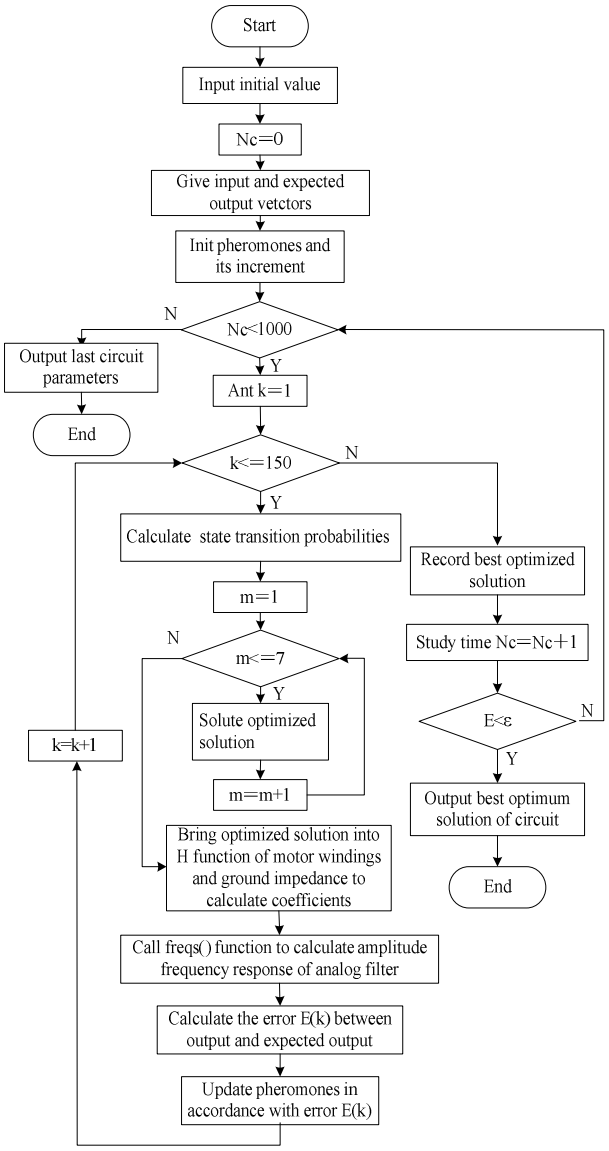

Fig.4 Setting circuit parameters flowchart by ACA algorithm

Based on experience and experiment result, we have following conclusion about ACA parameter selection: maximized number of loops NcMAX=1000, duration indices of residue information ρ=0.7, total pheromone Q=700, number of ants M=150, deviation E is limited to 0.1 (the smallest error allowed by algorithm). At the beginning, the original pheromone of each element in the set $\tau_j(Q_{P_i})(t)=3$ （$1 \leqslant j \leqslant N$） and $\Delta\tau_j(Q_{P_i})=0$, put all the ants into the formicary. Each ant choose the solution space according to state transition probability, and then take the parameter each ant chose into the H function and get the vector coefficient. After that, use freqs() function to calculate the amplitude and frequency output response of simulated filter constructed by these vector coefficients, the frequency bandwidth of this function is 150KHz~30MHz. The pheromone of each ant will be adjusted by the difference of analytical output and simulate output. After all the ants reached food sources, record the deviation of optimized solution; if the deviation faces the requirement, stops calculating, or continue. If all 150 ants after 1000 loops of searching could not reach the requirement, we should reconsider whether ACA is suitable for this type of problems.

5 Experiment and simulation

5.1 Experiment analysis

In order to get the high frequency EMI model of motor, it is necessary to achieve the amplitude and frequency characters of resistance of motor through experiment. Then equal it into a lumped-parameter circuit to make the analytical impedance of equivalent circuits the same as tested impedance of windings. We adopted Agilent 4249A precision impedance analyzer produced by Agilent Technology to test the impedance of motor. Its scale range is from 40Hz to 110MHz, covered the frequency bandwidth talked in this paper. Use that analyzer to test the short and open circuit impedance of XQ-7A2 separately excited DC motor. The testing principle showed in figure 5 (a) and (b).

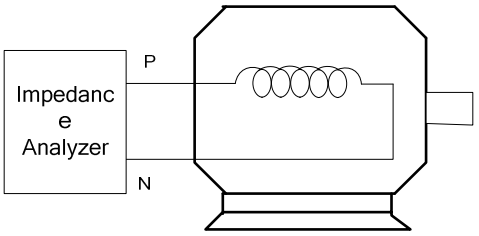

(a)

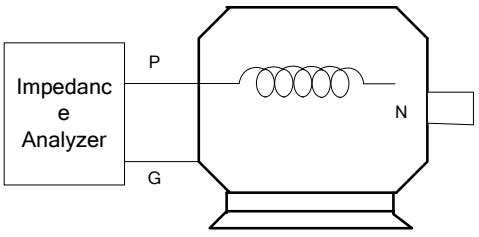

(b)

Fig.5 Test scheme of DC motor windings

Figure 6 (a) and (b) showed the test result of amplitude and frequency characters of short and open circuit impedance when DC motor operates in 150KHz ~ 30MHz frequency bandwidth.

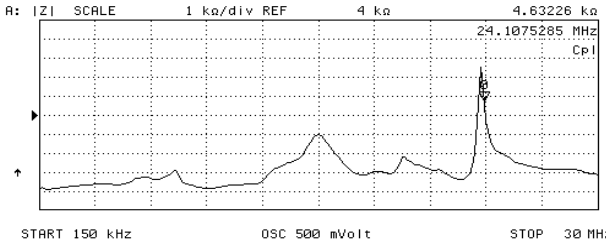

(a) Short circuit impedance

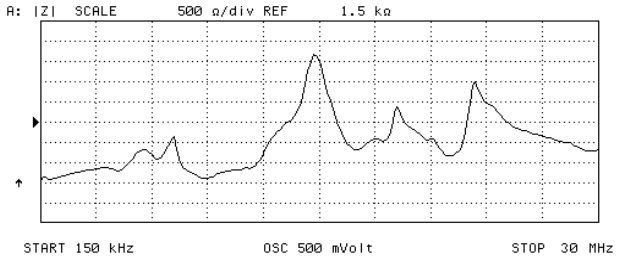

(b) Open circuit impedance
Fig.6 Comparison of DC motor windings characters

From the figure we found it is necessary to take the parasitic parameters related with common-mode signals inside the motors into account when setting up the high frequency common-mode equivalent circuit of separately excited DC motor.

5.2 Analysis of high frequency model of DC motor

In order to achieve the parameters of equivalent circuit, we adopted ACA to optimize the selection of parameter group. The training curve showed in figure 7. After 200 times of training, the result reached the accuracy requirement. The parameters of output equivalent circuit showed in table 1.

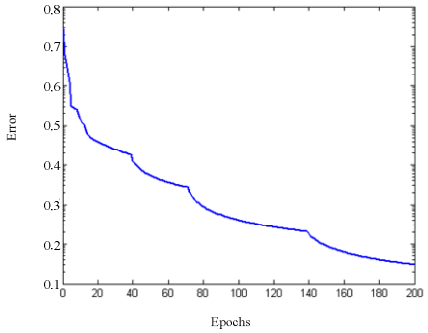

Fig.7 Training curve of ACA algorithm

Table 1 Setting DC motor equivalent circuit parameters by ACA algorithm

Parameters	Resistance		Capacitor/pF			Inductance/μH	
	R_a/m Ω	R_r/K Ω	C_a	C_r	C_f	L_a	L_r
Value	21.3	39.8	22	424	210	12.1	1.6

Comparison of simulate and test result of short and open circuit impedance showed in figure 8 (a) and (b).

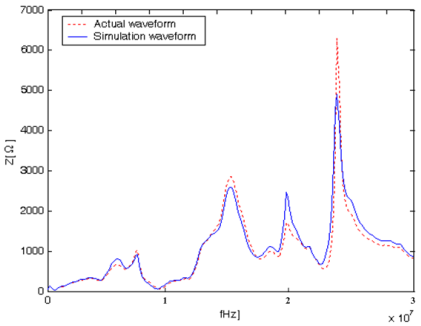

(a) Short circuit impedance

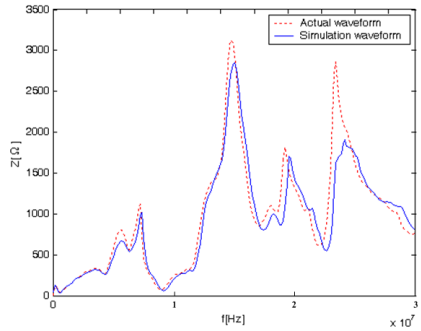

(b) Open circuit impedance
Fig.8 Compare the simulation result with experiment result of DC motor windings

From this figure we found that in high frequency (higher that 20 MHz), the difference between simulated and tested result is higher than that in low frequency, however, in the whole frequency domain, the simulated and tested result of common-mode impedance for DC motor are quite similar. Consequently, the equivalent circuit which its parameters are selected by Ant Colony Algorithm would reflect the common-mode impedance of separately excited motors correctly.

Figure 9 shows the difference between simulated and experiment error of short and open circuit impedance. It is clear that for the frequency higher than 20MHz, the error of simulated result is bigger than that of experiment result, since in high frequency the dielectric constant, permeability and other parameters of the medium inside motors are

function of frequency, not constant. That makes the parasitic capacity and inductance is not constant in the whole frequency. Accordingly, it will cause simulation error in high frequency that adopted constant value of parasitic capacity and inductance in the model [14].

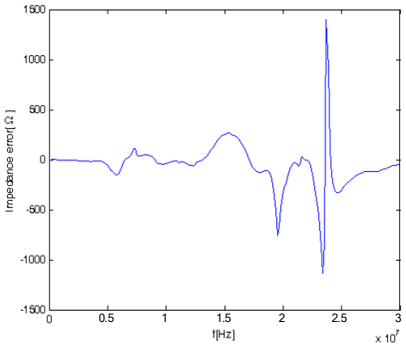

(a) Short circuit impedance

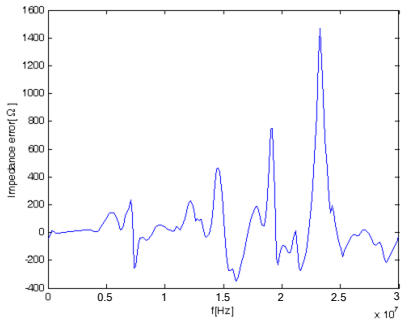

(b) Open circuit impedance

Fig.9 Error curve of simulation result

5.3 Algorithm comparison

We could verify the accuracy of ACA relative to greedy algorithm when algorithm is used to optimize parameters. Figure 10 shows the error result of different algorithm. We could find the error developing trend of greedy algorithm and ACA is similar, but the error of greedy algorithm is far more than that of ACA. The error of ACA is smaller than 1500 Ohm, but that of greedy algorithm is nearly 150k Ohm at the point of maximum error in short circuit impedance simulation, while the maximum error are 1600 Ohm and 160k Ohm in open circuit impedance simulation, respectively. So ACA is more suitable for the application of parameter optimization.

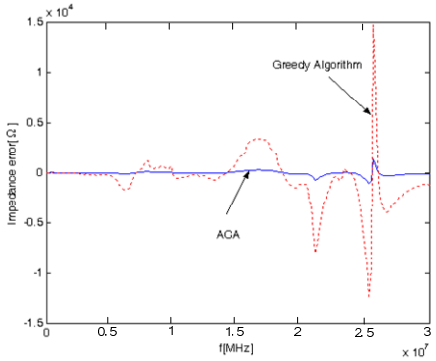

(a) Short circuit impedance

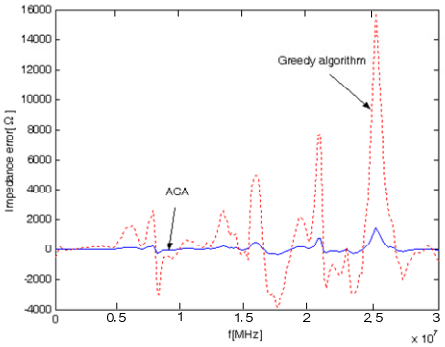

(b) Open circuit impedance

Fig.10 Error comparison of different algorithm

6 Analysis and simulation of separately excited DC motor

6.1 Analysis of interference source

When separately excited DC motors operation, since during the steering process, the terminal voltage and current of motor will generate periodic pulsation, there would be sufficient high frequency component of voltage in motor [15]. Figure 11 shows the equivalent circuit of steering process of DC motor. Set up the function of steering current and conducted interference source based on this equivalent circuit, then use numerical method MATLAB to get the interference solution in time domain [16].

Figure 11 takes the steering process with one group of brushes as example to analyze. The black rectangular on top and bottom are brushes. The state showed in figure is mutation state of steering component; as the rotation direction of armature windings marked in figure, the coil x and n are in the state of steering. As a result, R_s and L_s are the coil resistance and leakage inductance in two series branches, respectively. i_s is steering current of mutation component, since the circuit is symmetric,

it is sufficient to analyze one branch only. r_x and r_y are contact resistance between brush and two commutating segments, respectively; meanwhile, i_x and i_y are the current flows into commutating segments through brush, respectively. Two u_a branches are the two paralleled armature winding branches and u_a is the back electromotive force of armature branch, and i_a is the current in this branch.

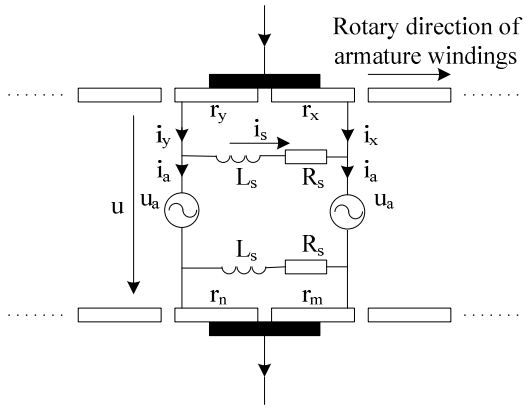

Fig.11 Equivalent circuit of DC machine commutation

According to Kirchhoff law, the voltage function of brush circuit showed in top of figure 6 can express as:

$$L_s \frac{di_s}{dt} + R_s i_s - r_x i_x + r_y i_y = 0 \tag{5}$$

$$i_x = i_a - i_s \tag{6}$$

$$i_y = i_a + i_s \tag{7}$$

When motor operating, the total outside voltage drop is composed by the contact voltage drop of the pair of brush u_c and the back electromotive force of the branch u_a, accordingly:

$$u = u_c + u_a \tag{8}$$

Based on electric machine theory, the back electromotive force of armature u_a is a certain constant when the motor rotates stable. Accordingly, the effect from u_a to conducted electromagnetic interference is negligible. That reveals the transient voltage when motor operating mainly comes from the contact voltage drop of brushes, especially by the end of the commuting process. The acute changes of contact voltage drop become the main resource of conducted interference in the motor. From figure 6 we found:

$$u_c = r_x i_x + r_y i_y \tag{9}$$

Suppose the contact between commutating segment and brushes is ideal, the contact resistance is:

$$r_x = R_d \frac{T_k}{T_k - t} \tag{10}$$

$$r_y = R_d \frac{T_k}{t} \tag{11}$$

Where R_d is the contact resistance when commutator contact with brush completely, T_k is the mutation period of DC motor, expressed as:

$$T_k = \frac{b_k}{v_k} = \frac{b_k}{v_a \frac{D_k}{D_a}} \tag{12}$$

Where b_k is the width of commutator. D_k and D_a are the diameter of commutator and armature, respectively. v_k and v_a are the linear velocity of the surface of commutator and armature, respectively [17]. Here the rated speed of motor is 1400 rpm, then take parameter D_k=360mm, b_k=100mm into equation (12), get the rated operation steering period is around 38.4 ms.

Since during the commuting process of DC motor, the transient current affects seriously to sensitive components, the effect from voltage drop is negligible and equation(5) is changed into:

$$L_s \frac{di_s}{dt} - r_x i_x + r_y i_y = 0 \tag{13}$$

Take (6), (7), (10) and (11) into (13), we have the function of commuting current i_s in time domain:

$$L_s \frac{di_s}{dt} = (\frac{T_k}{t} - \frac{T_k}{T_k - t}) R_d i_a - (\frac{T_k}{T_k - t} + \frac{T_k}{t}) R_d i_s \tag{14}$$

6.2 Simulation of interference source

Equation (14) is a typical first order differential equation and we can use solution command ode45 in MATLAB to get the i_s in time domain. Set up the starting steering current $i_s(0)$=10A, steering period T_k=38.4e-3s, time slot t=0.5e-7s, from former simulation result, we have the parameters of motor: L_s=121μH，R_d=21.3mΩ，i_a=10A. With the help of above, we have the solution of steering current is in time domain, and the curve showed in figure 12.

From the commutating current we could see that the current changed rapidly during the steering process, and this rapid change would cause transients of contact voltage between brush and commutator, even generate electric sparks.

Take (6), (7), (10) and (11) into (9), we have the function of contact voltage of DC motor:

$$u_c = (\frac{T_k}{T_k - t} + \frac{T_k}{t}) R_d i_a + (\frac{T_k}{T_k - t} - \frac{T_k}{t}) R_d i_s \tag{15}$$

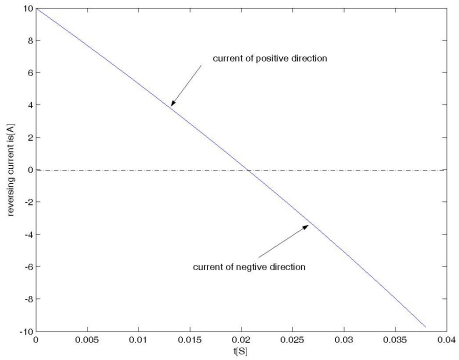

Fig.12 Changing waveform of commutating current

The first order differential function of contact voltage is:

$$\frac{du_c}{dt}=\left[\frac{T_k}{(T_k-t)^2}-\frac{T_k}{t^2}\right]R_d i_a+\left[\frac{T_k}{(T_k-t)^2}+\frac{T_k}{t^2}\right]R_d i_s \quad (16)$$

Take the solution of i_s in time domain got from numerical analysis into (15) and (16) we could get the solution of conducted interference emission source u_c in time domain. Figure 13 shows the curve of contact voltage u_c and changing rate of contact voltage du_c in time domain.

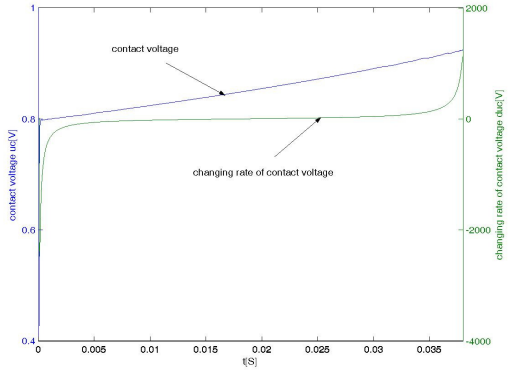

Fig.13 Changing curve of conducted interference source

The figure 13 reveals that the contact voltage changed as soon as the steering process starts, even after the process finished the contact voltage is still almost 1V, and the changing rate reached high voltage of 1500V by the end of the steering process and make it the main interference source in motor operation.

7 Special simulation and experiment analysis

The measurement of common mode conducted interference is to observe voltage on 50Ω resistance regulated by the linear impedance stabilizing network, LISN, through EMI receiver. There are 2 functions of LISN, one is to apply the 50Ω resistance in order to keep the comparability of measuring result, the common mode interference in certain frequency band could be observed through the voltage on that resistance; the other one is to divide the measured circuit and background noise on the power grid, in order to reduce the interference from power grid to result[18]. EMI receiver(ER55) will test EMI covering the frequency range from 9kHz to 2.8GHz, so it's ideally suited for measurement of electromagnetic interference in accordance with the requirements of FCC, CISPR, EN.

Connect motor windings with 12V DC power supply to make it operate stably, while serial connect LISN by the side with DC bus; its equivalent circuit is showed in figure 14. C_s is the coupled capacity from motor windings to the ground. Consequently, we get the curve of spectral with impedance of 50Ω to the ground and it is showed in figure 15.

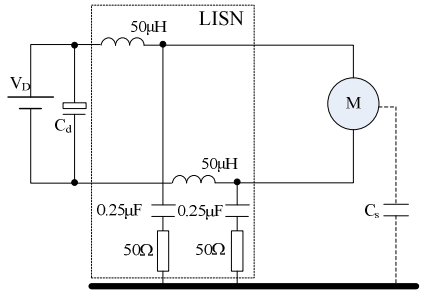

Fig.14 Equivalent circuit of common mode test

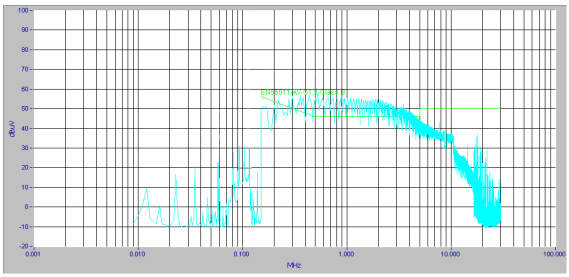

Fig.15 Actual spectrum measurement of DC machine

Figure 15 shows that without the control of power switch, common-mode conducted interference will be generated during the motor operates, especially in the frequency of 150kHz, the jamming intensity increased rapidly, and will hold a certain high intensity even reached 11MHz. This fact proves that DC will produce EMI when it works, and these interference will disturb other equipments through stray capacitance and ground. The green line in this figure is the requirement line of EN55011-AV-G1,2-Class B. We could find conducted EMI is above the requirement line of EN55011 in the

frequency range from 200kHz~4MHz. We may verify and optimize equivalent circuit model in accordance with this spectrum.

Figure 16 is the simulation model based on PSPICE circuit simulation software. In this figure, E1 is the high frequency interference source. This model adopted the activity simulation model in PSPICE. Activity simulation model is an extension of traditional controlled source described by mathematical calculation. Common activity models are saved in ABM.olb. In the simulation result showed in figure 13, the high frequency interference source of DC motor is modelled by GTABLE. Input the high frequency interference source in this model as the controlled source. Meanwhile, set a probe on the terminal of 25Ω resistance which represents LISN, then set up the analysis type as alternating analysis in setting window, and the scale range as 150KHz~30MHz[19-20].

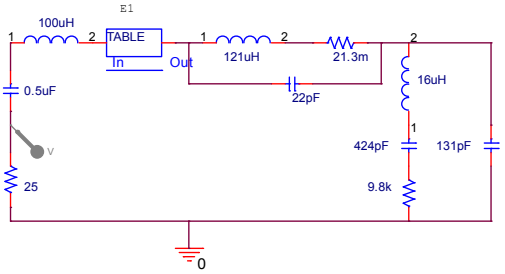

Fig.16 Model of circuit simulation

Figure 17 shows the comparison of simulated and experiment spectrum of LISN side common-mode voltage from PSPICE circuit simulation software. From the comparison we could find that simulated spectral curve could follow the experiment one correctly, proved the accuracy of the DC motor model and analysis of interference source.

8 Conclusion

Contemporary research about the equivalent circuit of separated excited DC motor in all EMC frequency is not sufficient. The work this paper accomplished was to research the high frequency common-mode equivalent circuit of separately excited DC motor based on the research of inner principle of DC motor and steering process, and determine the parameters by Ant Colony Algorithm. This equivalent circuit could be used for analysis and prediction of the motor side common-mode conducted EMI emission power and EMI current. Furthermore, the similarity of simulation and experiment result has proved its correctness.

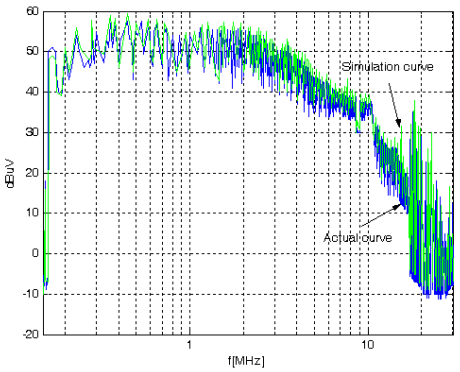

Fig.17 Spectrum contrast between simulation and experiment of common mode conducted interference in DC machine

Acknowledgement

This work is partially supported by Science & Technology Research Project of Heilongjiang Province(11551075) and Youth Foundation of Harbin University of Science & Technology(2009YF004). Thanks for foundation committee. My deepest gratitude goes foremost to Professor Wang Xudong, my supervisor, for his constant encouragement and guidance. He has walked me through all the stages of the writing of this thesis. Without his consistent and illuminating instruction, this thesis could not have reached its present form. Second, my thanks would go to my beloved family for their loving considerations and great confidence in me all through these years. Last, I also owe my sincere gratitude to my friends who gave me their help and time in helping me work out my problems during the difficult course of the thesis.

References:

[1] Nobuyoshi Mutoh, A Suitable Method for Ecovehicles to Control Surge Voltage Occurring at Motor Terminals Connected to PWM Inverters and to Control Induced EMI Noise, *IEEE Transactions on vehicular technology*, Vol.57, No.4, 2006, pp.2089-2098.

[2] G.M. Cheng, J.C. Waite, Minimization and Cancellation of Common Mode Currents, Shaft Voltages and Bearing Currents for Induction Motor Drives, *IEEE Transactions on Industrial Electronics*, Vol.53, No.5, 2006, pp. 1127-1132.

[3] Moreau M., Idir N. Le Moigne P., Utilization of a behavioured model of motor drive systems to predict the conducted emissions, *IEEE*

Power Electronics Specialists Conference, 2008, pp.4387-4391.

[4] Shan Chaolong，Ma Weiming，Wang Tiejun ，et al．Conducted EMI analysis and modeling of DC power supply with an inverter load, *Journal of Naval University of Engineering*，Vol.15, No.1, 2003, pp.1-5.

[5] Riehl R.R., Filho E.R., A simplified method for determining the high frequency DC motor equivalent electrical circuit parameters to be used in EMI effect, *International Conference on Electrical Machines and Systems*, 2007, pp.1244-1246.

[6] J. Benecke, S. Dickmann, Inductive and capacitive couplings in DC motors with built-in damping chokes, *17th International Zurich Symposium on Electromagnetic Compatibility*, Singapore, 2006, pp.182-189

[7] Jens Benecke, Andre Linde, Stefan Dickmann, Automatic HF Model Generatioin and Impedance Optimization for Low Voltage DC Motors, *Proceedings of the 2008 International Conference on Electrical Machines*, Vilamoura, Portugal, 2008, pp.134-142.

[8] Wang Lei, Wu Qidi, Ant System Algorithm in Continuous Space Optimization, *Control and Decision*, Vol.18, No.1, 2003, pp.45-48.

[9] Jennings A.L., Ordonez R., Ceccarelli N. , An Ant Colony Optimization using training data applied to UAV way point path planning in wind, *2008 IEEE Swarm Intelligence Symposium*, Saint Louis, USA, 2008, pp.781-788.

[10] Siqing Sheng, Jing Li, Study of reactive power optimization based on Artificial Immune Ant Colony Algorithm, *Electric Utility Deregulation and Restructuring and Power Technologies*, 2008, pp.2311-2315.

[11] Yiguang Chen, Xin Gu, Yonghuan Shen, Shengzhi Xing, Optimization of Active Power Filter System PI Parameters Based on Improved Ant Colony Algorithm, *IEEE International Conference on Mechatronics and Automation*, Luoyang, China, 2006, pp.93-100.

[12] Yuan Mingxin, Sunan Wang, Li Pengkun, A model of ant colony and immune network and its application in path planning, *2008 3rd IEEE Conference on Industrial Electronics and Applications*, Singapore, Singapore, 2008, pp.1034-1041.

[13] Wei Gao, New computational model from ant colony, 2*007 IEEE International Conference on Granular Computing*, San Jose, USA, 2007, pp.23-32.

[14] J. Benecke, S. Dickmann, Analytical HF model of a low voltage DC motor armature including parasitic properties, *IEEE International Symposium on EMC*, Honolulu, USA, 2007, pp.1152-1161.

[15] A.Boglietti, A.Cavagnino, M.Lazzari, Experimental High Frequency Parameter Idetification of AC Electrical Motors, *IEEE Transactions on Applications*, Vol.49, No.3, 2005, pp.5-10.

[16] J.S.Lai, X.D.Huang, E.Pepa, S.T.Chen, Inverter EMI Modeling and Simulation Methodologies, *IEEE Transactions on Industrial Electronics*，Vol.53, No.3, 2006, pp.736-744.

[17] R. Kahoul, P. Marcha, Y. Azzouz, B. Mazari, HF model of DC motor impedance EMC problems in automotive applications, *EMC 2008 IEEE International Symposium on*, Detroit, USA, 2008, pp.542-550.

[18] T.Williams, G.R. Orford, Best practice use of the CISPR AMN/LISN, *International Exhibition on Electromagnetic Compatibility*, 1999, pp.173-179.

[19] Saritha B., Janakiraman P.A., PSPICE simulation of current control of an electronically commutated motor, *Proceedings of the IEEE India Annual Conference*, India, 2004, pp.597-600.

[20] Purschel M. PSpice simulation of the power stage for DC brush motors using state of the art power MOSFETs, I*EEE Vehicle Power and Propulsion Conference*, 2009, pp.1567-1572.